

Schoch Effect in Topological Phononic Crystals

Yafei Cao^{1, a}, Yuanwei Yao¹, Huiping Feng¹

¹School of Physics and Optoelectronic Engineering, Guangdong University of Technology, Guangzhou 510006, China

^a569771773@qq.com

Abstract: This article investigates the Schoch negative displacement phenomenon at the interface between two-dimensional topological acoustic materials and traditional materials. The results show that a negative Schoch displacement occurs at the frequency of the Dirac point in the phononic crystal. At this point, the reciprocal of the effective bulk modulus of the phononic crystal tends to zero, making it an acoustic metamaterial with a refractive index close to zero. At the same time, the maximum value of the effective impedance of the phononic crystal and the real part of the reflection coefficient undergo a 2π phase transition at the corresponding frequency. When the phononic crystal is spliced into a topological supercell structure, a larger negative Schoch displacement is observed. This study demonstrates that topological phononic crystals can achieve negative Schoch displacement. The negative Schoch displacement realized in this article provides a new theoretical reference for designing acoustic devices based on interface waves.

Keywords: Schoch shift, Effective parameters, Phononic crystal.

1. Introduction

When a sound wave is incident on the interface between two media and undergoes reflection, the actual reflected beam is offset from the geometrically predicted reflected beam by a certain positive or negative amount, which is known as the Schoch displacement. This phenomenon is referred to as the Schoch effect [1]. The Schoch effect was first discovered by Schoch in 1950 through shadowgraphy when observing the reflection of ultrasonic waves at an interface, which revealed a non-specular reflection phenomenon [2]. Subsequently, Bertoni and Tamir developed a unified approximate theory to explain this phenomenon [3]. Since 2000, scientists have focused on the Schoch effect in adjustable periodic structure materials. In 2003, Declercq et al. used the theory of non-uniform wave diffraction and a one-dimensional periodic brass-water structure to investigate the reflection of ultrasonic waves, obtaining simulation data that was consistent with experimental results [4]. In 2004, Declercq et al. extended the theory of non-uniform wave diffraction to acoustic diffraction with negative Schoch displacement [5]. The research results indicate that the Schoch effect is closely related to the generation of interface Stoneley waves. In 2009, Herbison et al. developed a new method using pulse waves instead of harmonic waves in time domain to quantitatively measure the Schoch displacement [6]. In 2014, Declercq conducted experimental research on the energy conversion of ultrasound waves when Schoch displacement occurred [7]. In 2017, Chen et al. introduced defects (overlayers) at the interface between conventional materials and phononic crystals and achieved a large positive Schoch displacement by adjusting the thickness of the overlayers [8]. In 2020, Liu et al. discovered a negative Schoch displacement by adding an appropriately thick overlayer at the interface between a two-dimensional acoustic material and water, and provided theoretical explanations and effective parameters of the structure through calculations [9-11].

Metamaterials have received significant attention due to their extraordinary physical properties that conventional materials lack, including the negative Schoch displacement of sound waves. With the trend towards miniaturization of

acoustic devices, Schoch displacement is a crucial consideration. In recent years, research on near-zero refractive index materials has become quite mature, both in the acoustic and optical domains. The Schoch effect was discovered through inspiration from the Guass-Hankel effect, and significant progress has been made in both theoretical and high-precision experimental devices regarding the Guass-Hankel effect. Based on the Guass-Hankel displacement, a dual-channel narrowband filter was proposed in [12]. The linearly polarized light incident on near-zero refractive index optical materials was theoretically deduced and simulated in [13]. The impact of different incident wave wavelengths and temperatures on the Guass-Hankel displacement of near-zero refractive index optical materials was investigated in [14]. A mechanism for adjusting the size of the Guass-Hankel displacement was implemented by covering a single layer of graphene with adjustable voltage on the surface of a near-zero refractive index optical material in [15]. By adding a thickness-adjustable covering layer between conventional materials and optical metamaterials and using the incident angle of the beam and the thickness of the covering layer as variables, a significantly negative Guass-Hankel displacement several times the size of the supercell was achieved under suitable thickness selection in [16]. However, there are currently no reports on the Schoch effect in more complex near-zero refractive index acoustic materials. In order to further investigate the Schoch effect in acoustics, based on the research methods and experimental conclusions of optical metamaterials in [17], this paper designs a model that effectively achieves negative Schoch displacement in near-zero refractive index acoustic metamaterials with different physical characteristics by controlling the scattering body rotation direction and the thickness of the covering layer water at different parameters. Furthermore, the connection between the Schoch effect and the band structure of metamaterials is studied, and negative Schoch displacement was obtained using acoustic materials with topological properties.

When electromagnetic waves propagate in optical metamaterials, the interaction between the waves and the metamaterials is characterized by the permittivity and

permeability of the medium[18]. On the other hand, when acoustic waves propagate in acoustic metamaterials, the interaction between the waves and the metamaterials is characterized by the acoustic parameters of the periodic composite medium, such as mass density and bulk modulus, and other parameters such as shear modulus can also be used to control the properties of acoustic metamaterials[19]. This results in acoustic metamaterials having more complex and interesting physical properties. The Goos-Hänchen displacement in optical metamaterials usually occurs in the frequency range of megahertz and above, and its displacement size has negligible impact on the precision of modern optical devices. However, the Schoch displacement in acoustic metamaterials usually occurs in the low-frequency domain and cannot be ignored for small to medium-sized acoustic devices that operate in this frequency range. In this study, the incident frequency of sound waves was selected in the range of 800-1000 Hz, and the size of the negative Schoch displacement reached up to 8 times the lattice constant. Therefore, studying near-zero refractive index acoustic metamaterials will have richer implications.

2. Calculation Model and Results

The model system used in this article consists of conventional materials and acoustic metamaterials, as shown in Figure 1(a). From top to bottom, they are composed of mercury, water, and acoustic metamaterials arranged periodically in water with two-dimensional triangular scattering bodies. Figure 1(b) shows a single unit cell of the acoustic metamaterial, with a lattice constant of a and a distance of R from the vertex of the triangular scattering body to the center. The material parameters used in the numerical simulation are as follows: the density of the scattering body is $\rho = 8.9 \times 10^3 \text{ kg/m}^3$, the Young's modulus is $E = 2.0 \times 10^{11} \text{ Pa}$, and the Poisson's ratio is $\mu = 0.29$; the density of water is $\rho_1 = 1.0 \times 10^3 \text{ kg/m}^3$, and the wave speed is $c_0 = 1490 \text{ m/s}$; the density of mercury is $\rho_2 = 13.6 \times 10^3 \text{ g/m}^3$, and the sound speed is $c_1 = 1400 \text{ m/s}$. In order to excite surface acoustic waves and leaky waves more easily, a covering layer of water material was added at the interface between the metamaterial and the mercury solution, and the thickness of the covering layer was chosen as h_0 . A Gaussian acoustic wave (half-width) was incident on the acoustic metamaterials at a 45° angle from the mercury solution, and the simulation tests were performed with the frequency f of the incident sound wave as a variable.

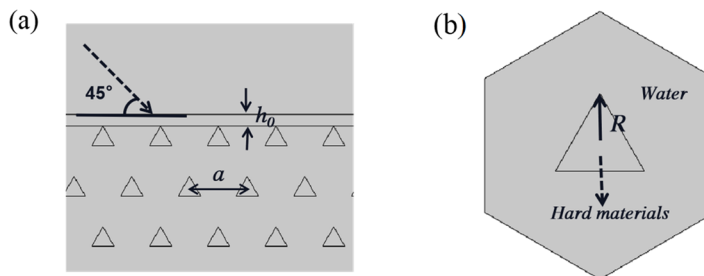


Figure 1. (a) The single cell of phononic crystal, in which the triangular scatterer is steel and the matrix is water; (b) Model structure, including mercury, water layer and steel from top to bottom

The reduced frequency at which the maximum negative Schoch displacement is generated by the incident Gaussian wave is denoted as F_S ($F_S = fa/c_0$). When $F_S = 0.567$ and the rotation angle of the scatterer is 30° , the reflected wave exhibits significant negative Schoch displacement and good Gaussian waveform, as shown in Figure 2(a). The solid black arrow represents the true propagation direction of the wave, while the dashed arrow represents the geometrically predicted direction. During the reflection process, a part of the energy flux reflects as surface waves and leaky waves that propagate respectively at the interface between mercury and water and in the covering layer. The position of the left reflected beam deviates significantly from the center of the incident beam,

indicating negative reflection dominated by surface waves and leaky waves. Meanwhile, a blank area appears between the two reflected beams, which is formed by the combined effect of the reflected beams and leaky waves that appear near the interface between the water layer and the superlattice [20]. When a large negative Schoch displacement occurs, a large number of backward leaky waves are generated near the interface between the water layer and the superlattice. It was also found that in this model structure, the reduced frequency F_S at which a large negative Schoch displacement is generated is located at the Dirac point of the band, as shown in Figure 2(b).

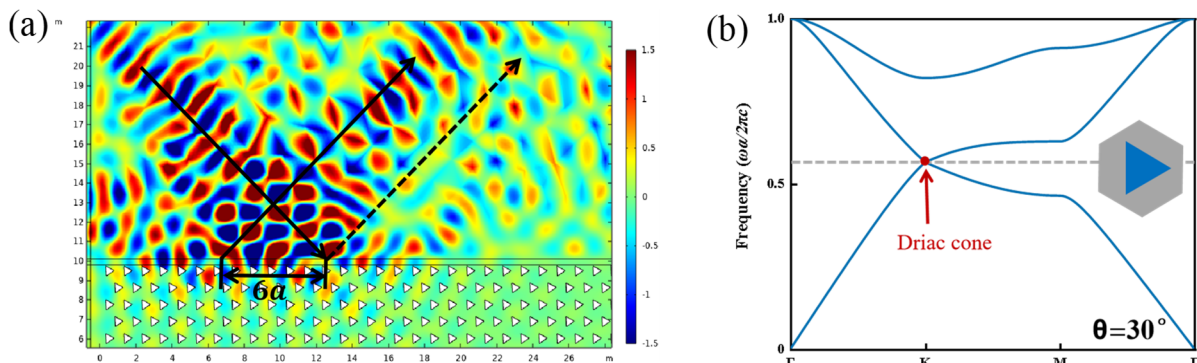


Figure 2. (a) The sound pressure field diagram with obvious negative Schoch shift; (b) the energy band structure of the material when Schoch shift occurs

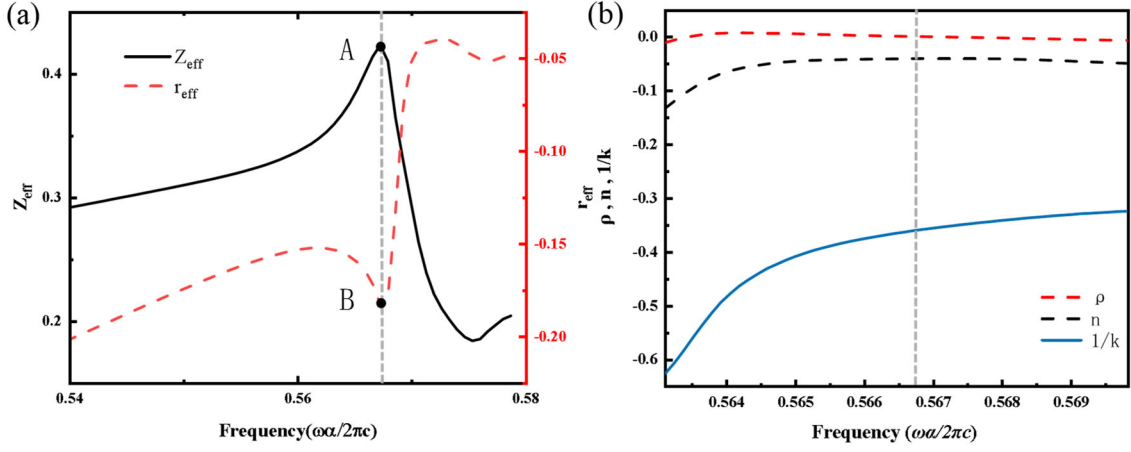


Figure 3. (a) with relative impedance (Z_{eff}) and reflection coefficient (r_{eff}) as a function of F ($F_s=0.567$); (b) for normalized frequencies in the structure, the effective refractive index (n), effective bulk modulus of the structure model The relationship between the reciprocal of the quantity ($1/k$) and the effective mass density (ρ)

To investigate the physical properties of the phononic crystal accompanying the appearance of negative Schoch displacement, the effective parameters of the periodic composite fluid-solid materials were referred to, and the variations of different physical parameters of the phononic crystal with respect to the reduced frequency F_s were calculated and obtained[20-25]. Figure 3(a) shows the variations of r_{eff} and Z_{eff} of the phononic crystal with respect to F_s when negative Schoch displacement occurs. Gray dashed lines parallel to the vertical axis are added as auxiliary lines in the figure. The abscissae of points A and B correspond to the reduced frequency at which negative Schoch displacement occurs. The peak values of r_{eff} and Z_{eff} of the phononic crystal appear at the same reduced frequency. The

impedance of the phononic crystal is related to the group velocity and density of phonons. Near the Dirac point, the group velocity of phonons is very small, and the density is very high, resulting in a very large impedance, which is consistent with the maximum value obtained at point A in Figure 3(a). Figure 3(b) shows the variation of n_{eff} , ρ_{eff} , and $1/k_{\text{eff}}$ with F_s . The abscissas of the auxiliary lines are the same as those in Figure 3(a). At $F_s=0.5668$, ρ_{eff} is close to and less than zero, $1/k_{\text{eff}}$ is less than zero, and the value of n_{eff} is close to and less than zero. Their relationship satisfies $n_{\text{eff}}^2 = 1/k_{\text{eff}} \times \rho_{\text{eff}}$, indicating that the phononic crystal can be regarded as an acoustic metamaterial with near-zero refractive index.

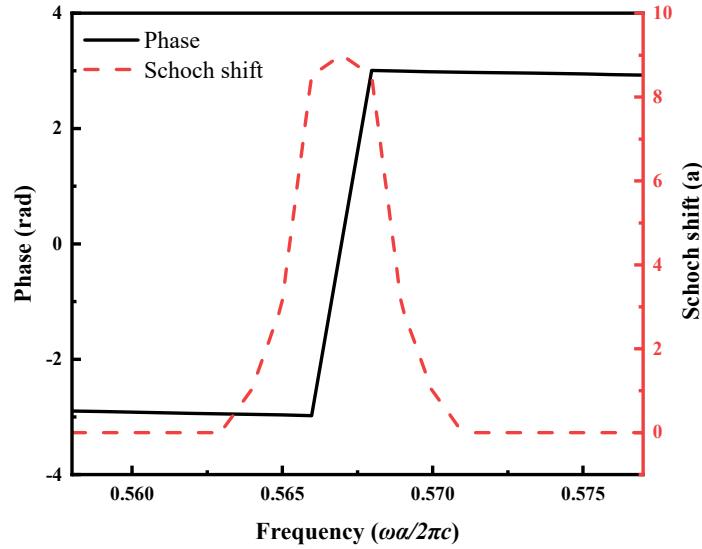


Figure 4. Schoch shift and phase variation of refractive index with frequency

Figure 4 shows the physical properties of the material when Schoch displacement occurs under the conditions of $R=0.3a$ and $F_s=0.567$. The black line indicates that the real part of the reflection coefficient has a sudden change in phase, and the phase difference before and after the sudden change is 2π rad. The red line indicates the corresponding number of Schoch at different frequencies. When $F_s=0.567$, the maximum negative displacement is obtained.

To investigate the relationship between the phononic crystal structure and negative Schoch displacement, the

scatterer R was changed to find the F_s corresponding to the peak reflection coefficient. Once the physical parameter characteristics were met, simulations were conducted to verify the occurrence of negative Schoch displacement at reduced frequencies. It was found that the physical parameter characteristics remained similar to those prior to the change in scatterer radius R . As shown in Figure 5 (a), the overall relationship between the reduced frequency F_s and the scatterer radius R was approximately linear, with F_s gradually decreasing as R increased. The red star point represents the

maximum Schoch displacement number obtained at different scatterer radii R . The characteristic frequency of Schoch displacement in phononic crystals with different structures always appeared at the frequency of the phononic crystal's Dirac point, with the r_{eff} and Z_{eff} of materials at this characteristic frequency appearing at their maximum. Following the observed phenomenon, for topological phononic crystals, the frequency generating the maximum

Schoch displacement was the frequency of the phononic crystal's Dirac point.

At the same time, it is found that the number of negative Schoch displacement will also change when the angle of the scatterer is changed in Figure 5 (b). As shown in the figure, when the angle of the scatterer is 0° , there will be no negative Schoch displacement. When the angle of the scatterer is 30° and 60° , the maximum Schoch displacement can be obtained.

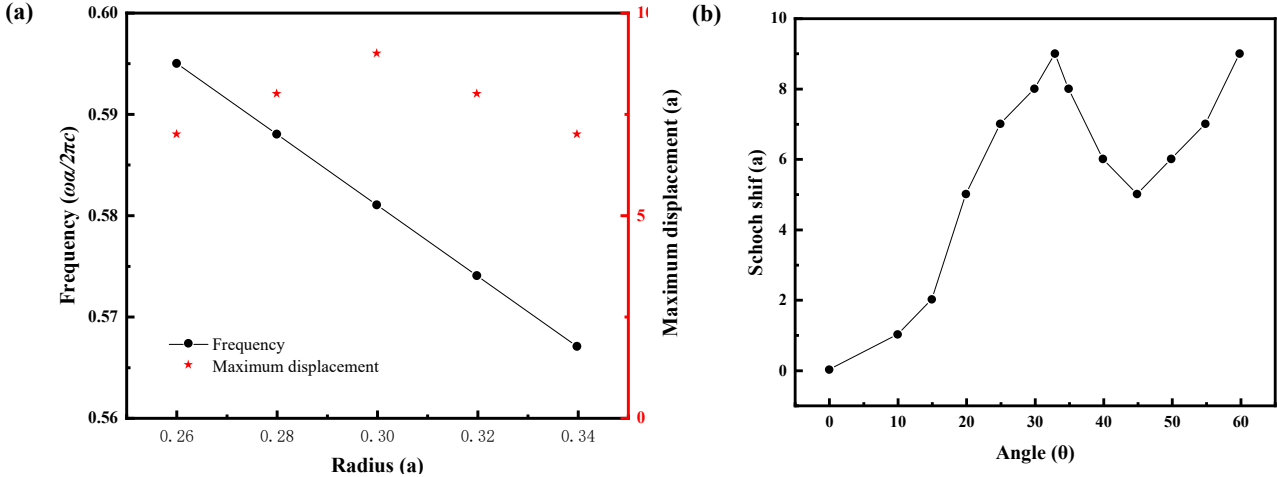


Figure 5. (a) When Schoch displacement occurs, FS changes with R , and the maximum number of Schoch displacement obtained by different radii (b) The number of maximum schoch displacements generated varies with the rotation angle of the scatterer

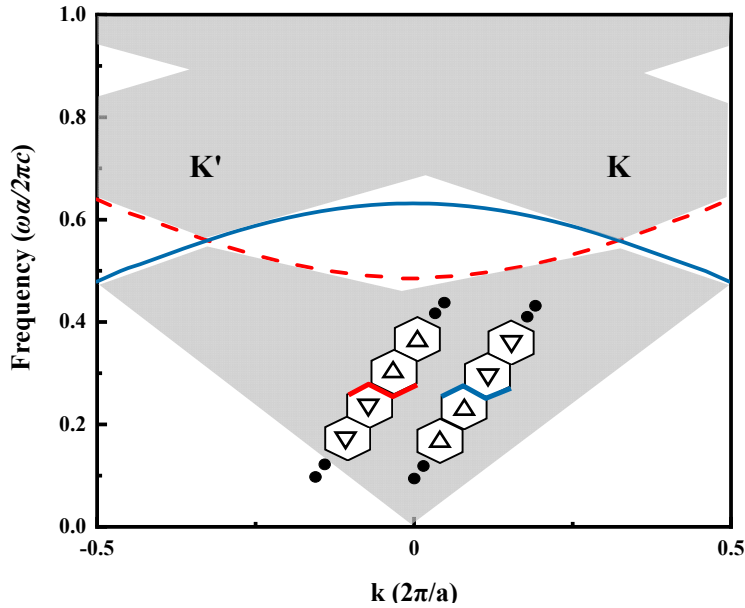


Figure 6. Dispersion curves of banded phononic crystals with different boundary types

On the boundary between structures with opposite topological valley phases, there exist topologically protected valley-polarized boundary states that are highly localized for acoustic waves[26]. The dispersion curve of a ribbon phononic crystal supercell composed of 20 upright trimer units and 20 inverted trimer units is shown in Figure 6, and the type of boundary formed between the two structures is a Z-shaped boundary, which can be defined as a positive boundary and a negative boundary .[27] In the band diagram, the red dashed line in the bulk band gap represents the helical boundary state transmitted along the negative boundary, while the blue solid line represents the topological boundary state transmitted along the positive boundary, and their group

velocities are exactly opposite. The formation of boundary states stems from the change in the topological valley Chern number of the different topological structures on both sides of the boundary, which can be expressed as:

$$2C^{(K',K)} = \pm 1 \times \text{sgn}(\Delta p) \quad (1)$$

The symbol Δp represents geometric perturbation, whose sign depends on the structure of the trimer in the primitive cell, specifically, the perturbations caused by the upright and inverted trimers satisfy the following: $\Delta p < 0$, $\Delta p > 0$.

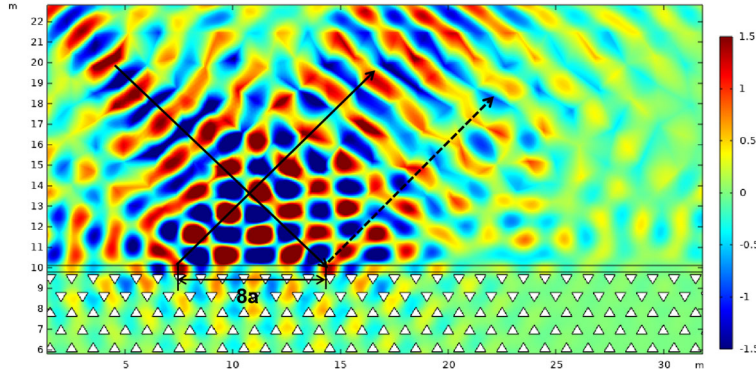


Figure 7. The sound pressure field diagram with obvious negative Schoch shift

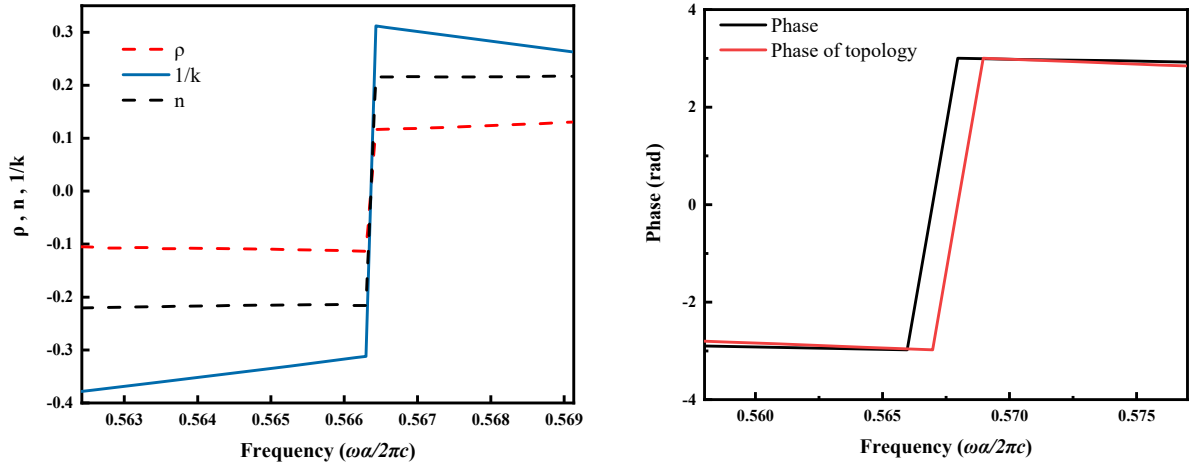


Figure 8. (a) Has the relative impedance (Z_{eff}) and reflection coefficient (r_{eff}) varying with F ($F_s=0.5655$); (b) For the normalized frequency in the structure, the effective refractive index (n), the reciprocal of the effective bulk modulus ($1/k$) and the effective mass density of the structure model (ρ) Relationship

As shown in Fig. 7, when $F_s = 0.565$, the reflected sound wave exhibits a significant negative Schoch displacement and a good Gaussian waveform. The negative Schoch displacement generated at this point is 8 times the lattice constant, which is larger and better than the negative displacement generated at the Dirac point. Fig. 8(a) shows the relationship between n_{eff} , ρ_{eff} , and $1/k_{\text{eff}}$ as a function of F_s , where ρ_{eff} is less than zero, $1/k_{\text{eff}}$ equals zero, and the value of n_{eff} is less than and close to zero. They satisfy the relationship $n_{\text{eff}}^2 = 1/k_{\text{eff}} \times \rho_{\text{eff}}$, and the phononic crystal can be regarded as a near-zero refractive index acoustic material at this point. Fig. 8(b) shows that the frequency of negative Schoch displacement in phononic crystals with topological

structure changes compared to before.

To verify the robustness of the topological structure, defects were introduced into the designed acoustic topological waveguide. As shown in Figures 9(a) and 9(b), the acoustic propagation characteristics of the waveguide with defects are essentially similar to those of the defect-free waveguide. Cavity defects with a random distribution and bent defects (achieved by removing the corresponding trimer units) were introduced into the phononic crystal. From the corresponding acoustic pressure maps, it can be observed that the resulting Schoch displacement is robust for both types of defects, as the presence of these defects has little effect on the generation of the Schoch displacement.

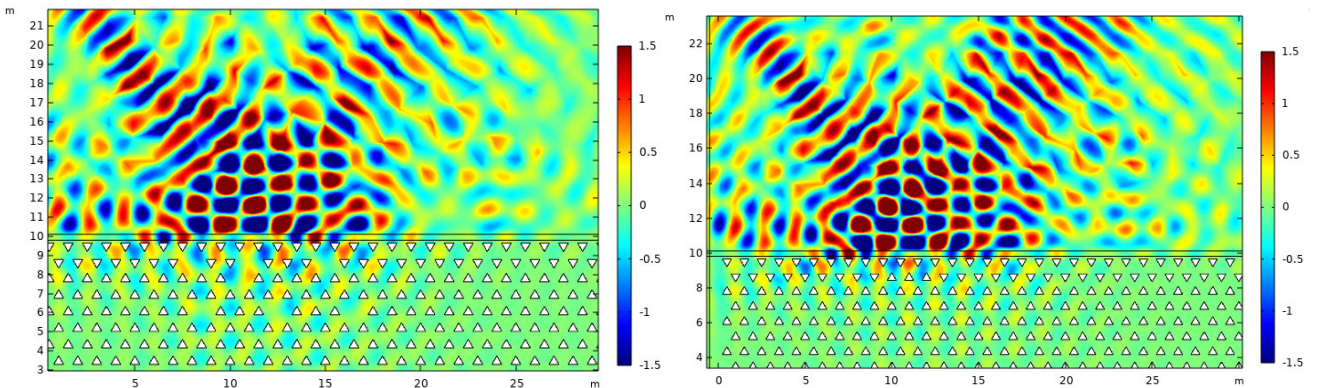


Figure 9. (a) Translates to "randomly distributed cavity defects were introduced; (b) Translates to randomly distributed bending defects were introduced (by removing the trimer unit at the corresponding position).

3. Summary

This article investigates the negative Schoch displacement at the interface between two-dimensional acoustic materials with topological properties and conventional materials. By adding a water cover layer at the interface between conventional materials and acoustic metamaterials, and selecting appropriate thickness parameters, a large negative Schoch displacement is achieved at the Dirac point frequency of the phononic crystal. The calculation results show that an appropriate cover layer thickness can induce part of the energy flux of the reflected beam at the interface to enter the cover layer and be converted into backward propagating leaky waves, thereby obtaining a negative Schoch displacement at the wavelength scale (meter-level) in the low-frequency domain. The occurrence of a large negative Schoch displacement is accompanied by several physical characteristics, including the reciprocal of the effective bulk modulus of the metamaterial approaching zero, making it an acoustic material with near-zero refractive index; the maximum value of the effective impedance of the metamaterial and the maximum value of the reflection coefficient almost coincide at the same reduced frequency; the real part of the reflection coefficient phase has a 2π rad phase change at the corresponding reduced frequency; the reduced frequency at which the negative Schoch displacement occurs is located at the Dirac point of the phononic band. A negative Schoch displacement is also obtained by topologically splicing the phononic crystals, which results in a larger negative displacement up to eight times the lattice constant. This study not only enriches the research results on Schoch phenomena in sound waves but also provides theoretical reference for designing acoustic devices based on interface sound waves.

References

- [1] Schoch A. Lateral displacement of a totally reflected beam in ultrasound waves[J]. *Acustica*, 1952, 2: 18-19.
- [2] Bertoni H L, Tamir T. Unified theory of Rayleigh-angle phenomena for acoustic beams at liquid-solid interface[J]. *Applied Physics A*, 1973, 2(4): 157-172.
- [3] Gao J, Cheng J C, Li B. Propagation of lamb waves in one dimensional quasiperiodic composite thin plates: a split of phonon band gap [J]. *Applied Physics Letters*, 2007, 90(11): 111908.
- [4] Declercq N F, Degrieck J. Theoretical verification of the backward displacement of waves reflected from an interface having superimposed periodicity[J]. *Applied Physics Letters*, 2003, 82(15): 2533-2533.
- [5] Declercq N F, Degrieck J, Briers R, et al. Theory of the backward beam displacement on periodically corrugated surfaces and its relation to leaky scholte-stoneley waves[J]. *Journal of Applied Physics*, 2004, 96(11): 6869.
- [6] Herbison, S. W., Declercq, N. F., & Breazeale, M. A. (2009). Angular and frequency spectral analysis of the ultrasonic backward beam displacement on a periodically grooved solid. *Journal of the Acoustical Society of America*, 126(6), 2939-2948.
- [7] Declercq, N. F. (2014). Experimental study of ultrasonic beam sectors for energy conversion into lamb waves and rayleigh waves. *Ultrasonics*, 54(2), 609-613.
- [8] Yang, Z., Mei, J., Yang, M., et al. (2008). Membrane-type acoustic metamaterial with negative dynamic mass. *Physical Review Letters*, 101, 204301.
- [9] Liu X.D., Wn F., Yao Y.W., Zhang X. Study on the negative Schoch displacement of two-dimensional acoustic metamaterials with near-zero refractive index. *Acta Physica Sinica*, 2021, 70(12): 272-278.
- [10] Mei J, Ma G C, Yang M, et al. Dark acoustic metamaterials as super absorbers for low-frequency sound[J]. *Nature Communications*, 2012, 3: 756.
- [11] Shen H J, Wen J H, Yu D L, et al. Research on a cylindrical cloak with active acoustic metamaterial layers[J]. *Acta Physica Sinica*, 2012, 61: 4303 (in Chinese).
- [12] Chen F, Hao J, Li H G, et al. Double-channel narrowband filter based on Goos Hanchen shift[J]. *Acta Physica Sinica*, 2011, 60: 4223 (in Chinese).
- [13] Xu, Y. D., Chan, C. T., & Chen, H. Y. Goos Hanchen effect in epsilon-near-zero metamaterials. *Scientific Reports*, 5, 8681 (2015).
- [14] Lu, Z. R., Liang, B. M., Ding, J. W., et al. Goos Hanchen shift based on near zero-refractive-index materials. *Acta Physica Sinica*, 65, 4208 (2016) (in Chinese).
- [15] Fan, Y. C., Shen, N. H., Zhang, F. L., et al. Electrically tunable Goos Hanchen effect with graphene in the terahertz regime. *Advanced Optical Materials*, 4, 1824-1828 (2016).
- [16] He, J. L., Yi, J., & He, S. L. Giant negative Goos Hanchen shifts for a photonic crystal with a negative effective index. *Optics Express*, 14, 3024-3029 (2006).
- [17] Shadrivov, I. V., Ziolkowski, R. W., & Zharov, A. A. Excitation of guided waves in layered structures with negative refraction. *Optics Express*, 13, 481-492 (2005).
- [18] Lamkanfi, E., Declercq, N. F., Van Paepegem, W., et al. Numerical study of Rayleigh wave transmission through an acoustic barrier. *Journal of Applied Physics*, 105, 114902 (2009).
- [19] Mei, J., Liu, Z. Y., Wen, W. J., et al. Effective mass density of fluid-solid composites. *Physical Review Letters*, 96, 024301 (2006).
- [20] Mei, J., Liu, Z. Y., Wen, W. J., et al. Effective dynamic mass density of composites. *Physical Review B*, 76, 134205 (2007).
- [21] Enoch S, Tayeb G, Maystre D. Numerical evidence of ultrarefractive optics in photonic crystals. *Optics Communications*, 1999, 161: 171-176.
- [22] Zhang J L, Jiang H T, Enoch S. Two-dimensional complete band gaps in one-dimensional metal-dielectric periodic structures. *Applied Physics*, 2008, 92: 053104.
- [23] Felbacq D, Smaali R. Bloch modes dressed by evanescent waves and the generalized Goos-Hanchen effect in photonic crystals. *Physical Review Letters*, 2004, 92: 193902.
- [24] Felbacq D, Moreau A, Smaali R. Goos-Hanchen effect in the gaps of photonic crystals. *Optics Letters*, 2003, 28: 1633.
- [25] Wan Y H, Zheng Z, Kong W J, Zhao X, Liu Y, Bian Y S, Liu J S. *Opt. Express*. 20 (2012) 8998.
- [26] Enoch S, Tayeb G, Maystre D. *Opt. Commun.* 161 (1999) 171.
- [27] Zhang J L, Jiang H T, Enoch S, Tayeb G, Gralak B, Lequime M. *Appl. Phys. Lett.* 92 (2008) 053104.